Bull. Natn. Sci. Mus., Ser. E (Phys. Sci. & Engineering), 1, Dec. 22, 1978

Japanese Iron Meteorites: Chemical Composition and Microanalytical Observation of Kuga, Shirahagi, Tanakami and Tendo

By

Masako SHIMA

Department of Physical Sciences, National Science Museum, Tokyo,

Akihiko OKADA

The Institute of Physical and Chemical Research, Wako, Saitama,

Yoshihisa OMORI, Tetsuya MASUDA

Analytical Center, Shimadzu Seisakusho Ltd., Kyoto,

and

Yasunobu TANAKA

Tokyo Research and Application Laboratory, Shimadzu Seisakusho Ltd., Tokyo

I. Introduction

As is well known, iron meteorites are composed mainly of iron and nickel alloy, the so called metallic phase, but also contains several minerals such as troilite, FeS, schreibersite, $(Fe, Ni)_3P$, graphite, C, and some metal sulphides, phosphides, carbides and nitrides. These minerals are usually dispersed in the whole body of the iron meteorite but their size and distribution are not uniform.

When chemical composition of iron meteorites are discussed, only the abundances of elements in the metal phases are usually considered. This, however, of course does not give the real chemical composition of iron meteorites.

In this report, the chemical composition of elements in the metal phase of four iron meteorites, Kuga, Shirahagi, Tanakami and Tendo, is first described and then some examples of microanalytical observations of metal phases as well as inclusion minerals are presented.

II. Samples

Iron meteorites, Shirahagi and Tanakami were found in the 19th century. Chemical analyses of the main components, Fe, Ni, Co, Cu and P, were already made by Kondo (1895) and Kodera (see; Enomoto 1902, Kō 1899 and Otsuki 1900). Small pieces of these two meteorites were given to a couple of places of the United States of America a long time ago, and Tanakami was provided to the British

Museum, London, England. Further analysis of Shirahagi was performed by Wasson (1974), and that of Tanakami was done by Scott *et al.* (1973). They are classified chemically in Group IVA and IIIE respectively. The iron meteorite belonging to chemical group IIIE is rather rare. Moreover, these authors reported that Tanakami is a somewhat unusual coarse octahedrite, with its anomalous kamacite morphology and significant amount of carbides. We have the main mass, ~170 kg., of Tanakami in National Science Museum, but it is very hard to cut out a moderate size specimen for research purposes. For this reason, we could obtain only a somewhat limited analytical results for Tanakami.

The other two meteorites Kuga (Murayama, 1959 and 1965) and Tendo (Murayama, 1977) were found at the begining of the 20th century but were recognized as iron meteorites rather recently. There are neither analytical data nor microanalytical observations on these meteorites. Tendo is heavily oxidized and the main mass is still privately owned, and the owner provided us only a small end piece. Rust has grown along the boundary between metal crystals as well as inclusion minerals in the interior of the meteorite. Normally, Fe-Ni alloy with lower nickel content rust easily. Therefore, we expected that the values obtained as analytical data will be somewhat too low for Fe in Tendo.

III. Chemical Composition of Kuga, Shirahagi, Tanakami and Tendo

A. *Experimental*:

During the last year, experimental scope and analytical methods have been extended from time to time. Sample processing methods employed in this study are shown in Fig. 1 (a) and (b).

Before starting the dissolution procedure, all specimens were washed in dilute HCl. If there are any inclusion minerals such as troilite and phosphide, HCl treatment is useful to take out such inclusions. The specimens are then, rinsed with H_2O and acetone, and dried at room temperature.

The dissolution methods (a) and (b) were used for the analyses of the main component elements, Fe, Ni, Co, P, Cu and Cr by EDTA titration methods, atomic absorption and colorimetry. For the titration and colorimetry, ideally it is necessary to separate each element from Fe and the other elements. Separation by anion exchange resin column with HCl system was used for this purpose.

(a) About 1 g of metallic phase of meteorite was, after being washed and dried, dissolved in HNO_3. Excess acid was evaporated to dryness and HCl was added to the residue to decompose nitrate. The excess acid was again evaporated to dryness and HCl was added to it. This procedure was repeated a couple of times until NO_3^- was completely decomposed. The last residue was dissolved in concentrated HCl and the solution was poured into about 70 ml. of anion exchange resin, Dowex-1, X-8, 100~200 mesh, column, saturated in concentrated HCl. First solution, eluted

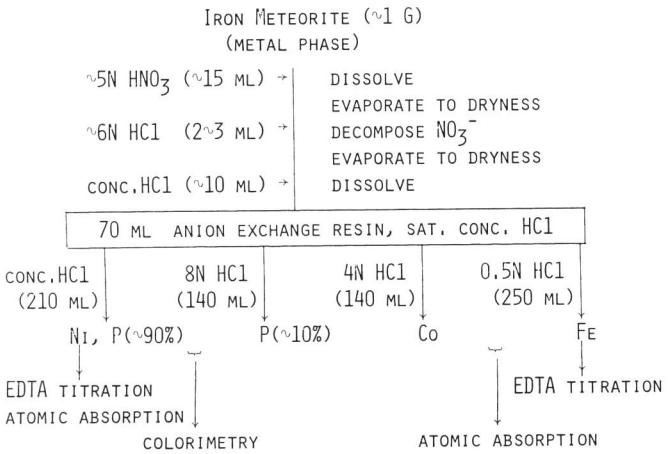

(a)

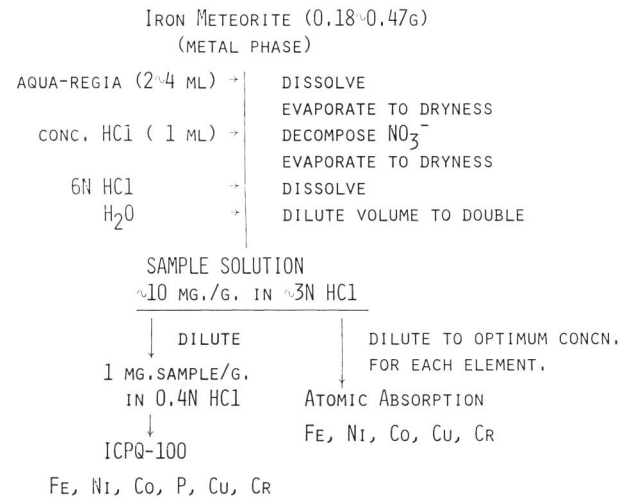

(b)

Fig. 1. Schematic Diagram of Chemical Treatment before Chemical Measurements.
(a) The dissolution method and chemical separation by anion exchange resin for the specimens (a).
(b) The dissolution method for the specimens (b).

by about 3 column volumes of concentrated HCl, contains Ni and ~90% of P. Next two column volumes of 8N-HCl elute the rest of P. Two column volumes of 4N-HCl remove Co from column, and the last 3.5 column volumes of 0.5N-HCl elute all Fe. From each fraction, excess acid was evaporated separately, and the optimum concentration of each element were prepared by diluting each fraction with

H_2O. Iron and Ni were determined by EDTA titration, and Fe, Ni, Co, Cr and Cu by atomic absorption, and P was measured by colorimetry.

(b) The cleaned metallic phase was dissolved in aqua-regia. After all nitrates were decomposed by HCl treatement, the residue was dissolved in HCl. A part of the solution was further diluted to carry out the atomic absorption measurements. Another solution was used for the analyses by ICPQ-100. The ICPQ-100 is an emission spectrometer equipped with a new excitation source, and inductively coupled radio frequency plasma, that is, argon plasma energized by radio frequency power of 27 MHz, 1.6 kW. The sample solution is blown into this flame as aerosol by argon gas. The advantages of ICPQ-100 are high sensitivity, high precision, good reproducibility, minimum interelement effect and linear relationship between intensity and concentration in the wide range of about 5 orders of magnitude, as the

Table 1. Chemical Composition of Iron Meteorites
(weight percent)

No.	sample taken	method	Fe	Ni	Co	Cr	Cu	P
Kuga								
(a)	1.0823	Tit.	87.24	9.97	—	—	—	—
		A.A. & color.*	84.36	9.36	0.58	≤0.002	0.011	0.290*
mean			85.80	9.68	0.58	≤0.002	0.011	0.290
Shirahagi								
(a)	1.0574	Tit.	90.51	7.59	—	—	—	—
		A.A. & color.*	90.17	7.41	0.40	0.034	0.015	0.0260*
(b)	0.4684	ICPQ-100	87.49	7.81	0.36	—	0.014	0.0296
		A.A. & color.*	88.70	7.92	0.39	0.028	0.015	0.0293*
mean			89.22	7.68	0.39	0.031	0.015	0.0277
Tanakami								
(a)	1.1222	Tit.	88.58	8.21	—	—	—	—
		A.A. & color.*	87.35	8.34	0.50	≤0.002	0.012	0.149*
(b)	0.1762	ICPQ-100	—	9.96	0.51	0.0059	0.015	0.160
		A.A. & color.*	86.74	10.21	0.53	0.0044	0.015	0.152*
mean**			87.80	8.52	0.50	0.0052	0.013	0.150
Tendo								
(a)	1.0625	Tit.	80.15	9.40	—	—	—	—
		A.A. & color.*	76.35	9.63	0.49	<0.002	0.017	0.310*
(b)	0.2801	ICPQ-100	74.85	8.13	0.42	0.0003	0.013	0.250
		A.A. & color.*	71.21	8.41	0.47	<0.002	0.013	0.247*
mean**			87.	8.89	0.54	0.0003	0.015	0.297

* measured by colorimetry.
** see text.

results of using a high temperature stable flame of about 9000 K. Further details of this apparatus are described by Imai *et al.* (1978).

B. *Results*:

Analytical results for main component elements in four iron meteroites, Kuga, Shirahagi, Tanakami and Tendo are tabulated in Table 1. Comparison of the present results for Shirahagi and Tanakami with the data already published is made in Table 2.

Table 2. Comparison of Present Work with Published Data

a) *Shirahagi*

elements	present work mean value	Kondo (1895)	Enomoto (1902) analyst, Kodera	Wasson (1974)
Fe (%)	89.22	93.52	89.467	—
Ni (%)	7.68	5.92	9.303	7.86
Co (%)	0.39	0.20	0.827	—
Cu (%)	0.015	—	0.138	—
P (%)	0.0277	—	0.064	—
C (%)	—	—	0.219?*	—
S (%)	—	—	0.219	—
Sn (%)	—	—	0.011?*	—
Ga (ppm)	—	—	—	2.19
Ge (ppm)	—	—	—	0.120
Ir (ppm)	—	—	—	2.4

b) *Tanakami*

elements	present work mean value	Ko (1899)	Otsuki (1900) analyst, Kodera	Scott *et al.* (1973)
Fe (%)	87.80	88.941	90.122	—
Ni (%)	8.52	8.651	8.560	8.94
Co (%)	0.50	0.594	0.623	—
Cu (%)	0.013	trace	trace	—
P (%)	0.150	0.425	0.441	—
Ga (ppm)	—	—	—	18.2
Ge (ppm)	—	—	—	34.4
Ir (ppm)	—	—	—	0.22

* These data are doubtful, probably contamination.

From Table 1, it is apparent that in Shirahagi, which is a fine octahedrite, the differences between different specimens are almost negligible, because of its fine-grained structure. Wasson's data for Ni, 7.86% (1974), also agree with ours, 7.68%, well whereas old data by Kondo (1895) is too low and by Kodera (Enomoto, 1902) is too high. For Tanakami, which is a coarse octahedrite, the differences of Ni content in different specimens are as high as ~20%. The reason is that the No. (b) speci-

men weighing only 0.18 g is too small in size compared with the coarse-grained structure of this meteorite. If we take for Ni in Tanakami the weighted mean value of No. (a) and No. (b) specimens taking account of their sizes, we obtain 8.52% which is in good agreement with the published data, 8.61% and 8.560% by Kodera (1899 and 1900) and 8.94% by Scott *et al.* (1973). As was described in the section on samples, Tendo is heavily rusted, and the rust is not evenly grown in the interior of the meteorite. Low Ni phase, less than 6% in Ni content, and the boundary around troilite and schreibersite inclusions usually rust easily. Thus, in order to obtain reasonable analytical data, an incremental correction of about 15% should be made for Fe and Co, and that of a few percent for P, but not for other elements such as Ni, Cr and Cu which are rather poor in such a rusty specimen (Shima and Honda, 1966a and b).

Plots of logarithmic P concentration versus Ni concentration for iron meteorites in chemical group III and IV, totally 213 in number are given in Fig. 2. Present data for Kuga, Shirahagi, Tanakami and Tendo given in this figure, indicate that they belong to chemical group IIIB, IVA, IIIE, and IIIA or B respectively.

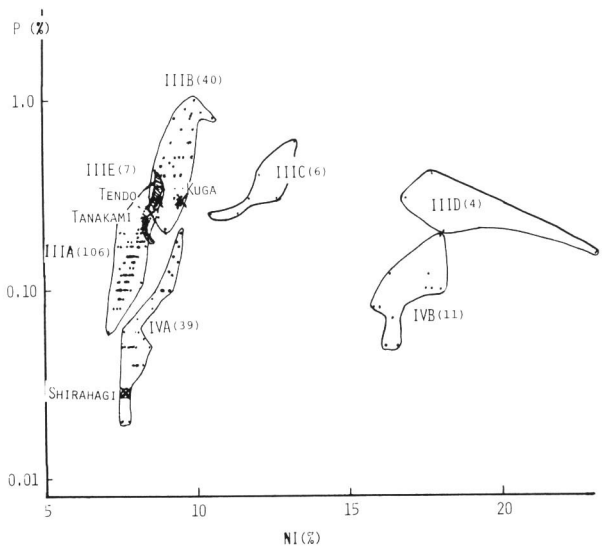

Fig. 2. The relationship between logarithmic concentration of P and Ni concentration.

This is confirmed that good analytical data of phosphorus should also become the indicator element of the chemical classification of iron meteorites beside Ga, Ge and Ir porposed by Wasson (1974).

IV. Microanalytical Observation of Kuga, Shirahagi, Tanakami and Tendo

A. *Experimental Method*:

Polished sections of meteorite samples for the microscopic investigation in the reflected light and electron probe microanalysis were prepared by the following procedure. A meteorite section was cut from the original meteorite sample with a diamond wheel. In sawing, cold nitrogen gas passing through liquid nitrogen was streamed onto both the meteorite sample and the diamond blade in order to avoid heating the sample. The meteorite section was then embedded in epoxy resin, and a flat surface was prepared by polishing successively with silicon carbide abrasives, 40 μ and 20 μ in particle size, and 10 μ alumina powder, followed by polishing with 1 μ and 0.3 μ alumina powders on wet lapping clothes. The surface of the sample was finally polished with 0.06 μ alumina, and was cleaned ultrasonically. No etching was done for the microscopic examination, because the polished sample were subsequently investigated by electron probe microanalysis. Mineral species were identified by the optical properties and by the qualitative X-ray microanalysis. The Debye method was also used for the mineral identification, by extracting mineral grains from the surface of the sample. Microchemical compositions and microstructures of each mineral were examined by the EMX-SM X-ray microanalyzer made by Shimadzu Seisakusho Ltd. A finely focused electron beam was bombarded on the polished sample coated with carbon layer, a few hundred angstrom thick, and the resultant characteristic X-ray emissions of major element were measured by the X-ray detection system. Accelerating voltage and sample current were 15 kV and 0.03 μA respectively.

B. *Results*:

Description of Kuga; Kuga is mainly composed of kamacite, α-Fe(Ni), and taenite, γ-Fe(Ni), and well-developed Widmanstätten structure is observed in the polished surface (Fig. 3). The plessite area is separated from the kamacite phase by

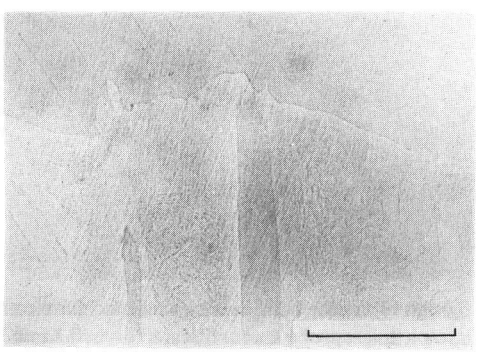

Fig. 3. Widmanstätten structure of Kuga. Scale bar is 0.2 mm long.

the rim of taenite, 0.03 mm wide in maximum, and the kamacite band width ranges generally from 0.54 mm to 0.66 mm. A metallographic feature characteristic of kamacite is the prevalent occurrence of Neumann bands resulting from mechanical twinning, and feathering of Neumann bands is commonly observed as shown in Fig. 4, indicating that Kuga has undergone a moderate degree of shock event (Heymann *et al.*, 1966). Schreibersite, ranging from 0.5 to 2 mm in size, occurs in accessory amount in the kamacite phase (Fig. 5). Troilite was not found in the small polished samples used in this study, but large troilite nodules ranging up to centimeter-size are present in the original sample of Kuga. Fig. 6 shows the

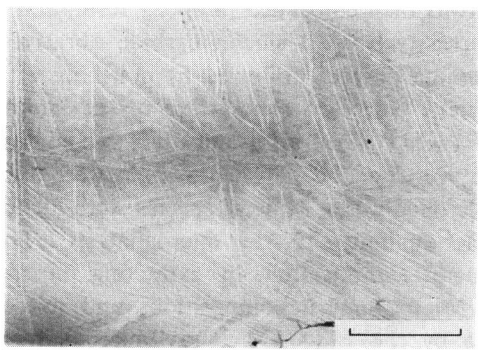

Fig. 4. Neumann bands found in kamacite of Kuga. Feathering is observed. Scale bar is 0.2 mm long.

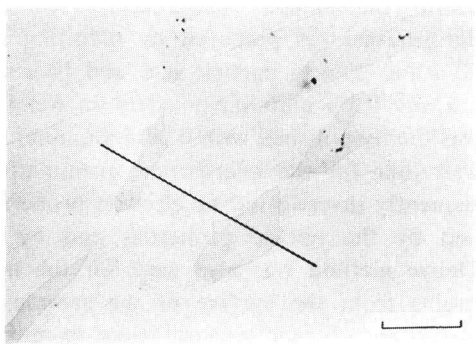

Fig. 5. Schreibersite inclusions in kamacite of Kuga. Electron microprobe analysis was carried out along the line (see: Fig. 7). Scale bar is 0.1 mm long.

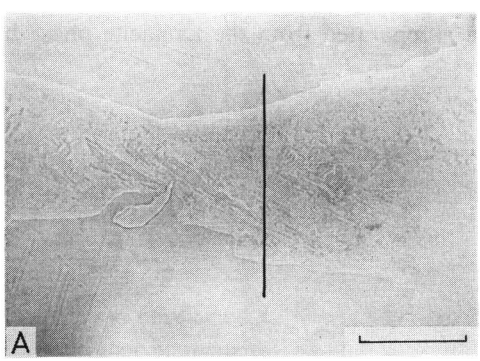

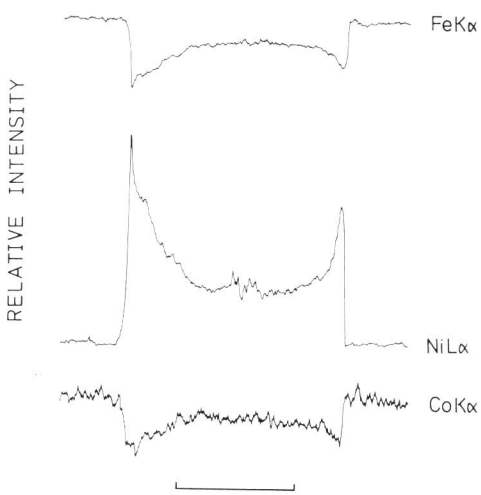

Fig. 6. A: Photomicrograph of taenite band in Kuga selected for electron probe microanalysis. The vertical line shows a microprobe track. Scale bar is 0.2 mm long.
B: FeKα, NiKα and CoKα profile across the taenite band. Scale bar is 0.1 mm long.

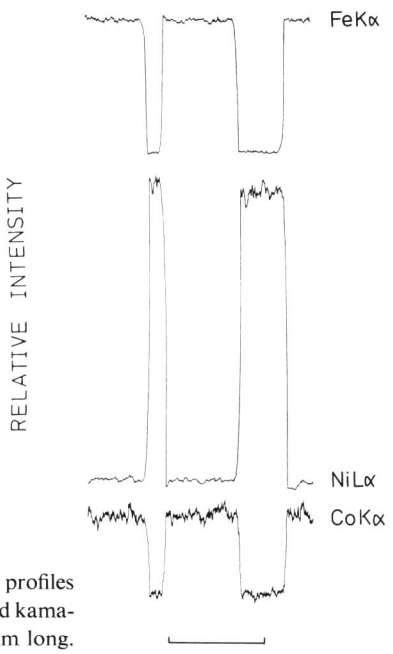

Fig. 7. FeKα, NiLα and CoKα profiles across schreibersite inclusions and kamacite in Fig. 5. Scale bar is 0.1 mm long.

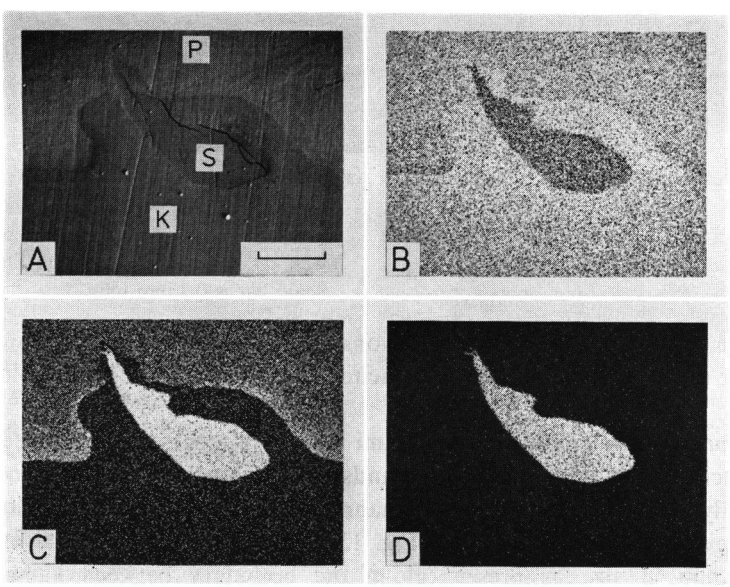

Fig. 8. A: Back-scattered electron image of schreibersite (S), kamacite (K) and Plessite area (P) of Kuga. Scale bar is 0.04 mm long.
B–D: FeKα, NiKα and CoKα images, respectively.

electron microprobe profile of Fe, Ni and Co distributions across the taenite band. The Ni-profile is typically M-shaped, while Fe distribution is inversely M-shaped, correlating with Co distribution. FeKα, NiKα, CoKα and PKα images and Fe-, Ni- and Co-profiles show that schreibersite is Ni-rich and Co-poor, and that it is chemically homogeneous from part to part in the interior of the grain (Fig. 7 and 8).

Description of Shirahagi; Shirahagi is essentially composed of kamacite, and contains small amount of taenite. Minute schreibersite grains, less than 0.03 mm in size, are present in the kamacite phase. The structure observed in the present specimen is unusual in that taenite occurs in linearly streched veins along one specific direction (Fig. 9). At a higher magnification, fine plessite structure is often observed in a much wider taenite vein. In the original sample, extremely deformed Widmanstätten structure is clearly observed (Fig. 10), and kamacite and taenite bands vary in width from part to part probably caused by severe deformation. The peculiar structure of Shirahagi probably arose from intense distortion by some external force as mentioned by Murayama (1953).

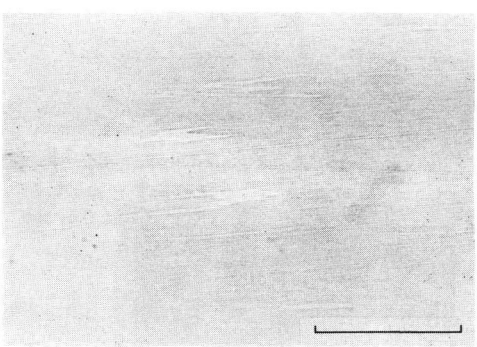

Fig. 9. Photomicrograph of a polished section of Shirahagi. Linearly stretched taenite veins are observed in kamacite. Scale bar is 0.05 mm long.

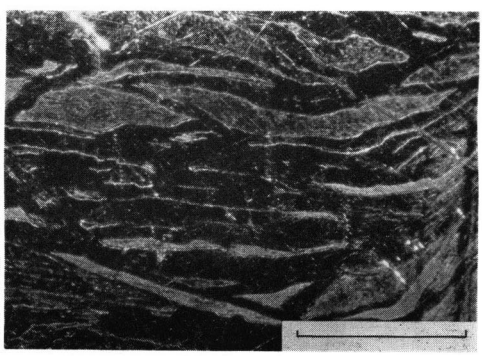

Fig. 10. Deformed Widmanstätten structure observed in the etched surface of the original Shirahagi sample. The photograph was taken under an oblique illumination. Scale bar is 0.2 mm long.

Fig. 11 shows Fe, Ni and Co variations across the taenite vein. Ni content is a little higher at the edge adjacent to kamacite, while Fe content is a little lower on the contrary.

Description of Tanakami; Tanakami shows a coarsely developed Widmanstätten structure (Fig. 12). Kamacite bands range from 1.0 to 1.7 mm in width, and are generally swelling in shape. Neumann bands are rare, but are distinctly observed in several grains of kamacite (Fig. 13). Schreibersite, fractured in shape and 0.1 to 0.9 mm in size, is present along the boundary between kamacite plates. Rhabdite-like grains are frequently observed dispersing in kamacite in the form of minute blobs, 20–30 μ in size, and micron-sized needles. Fig. 12 shows a rare mineral, ranging from less than 10 up to 50 μ in size, existing inside the plessite area. This

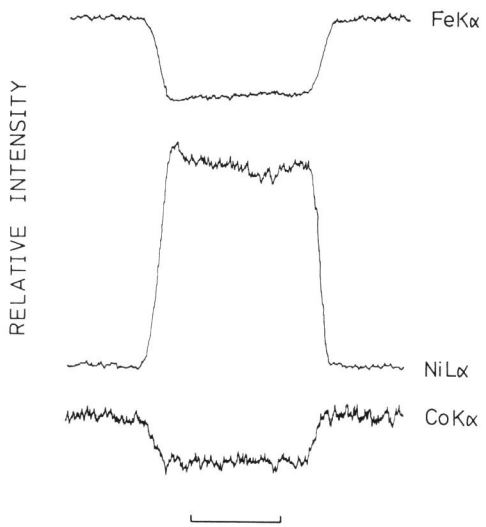

Fig. 11. FeKα, NiLα and CoKα profiles across taenite vein of Shirahagi. Scale bar is 0.005 mm long.

mineral shows an isotropic nature in polarized light and is composed mainly of iron and carbon (Fig. 14). These properties of the mineral suggest that it is likely a kind of iron carbide species, haxonite [$(Fe,Ni)_{23}C_6$], which is characteristic of IIIE iron.

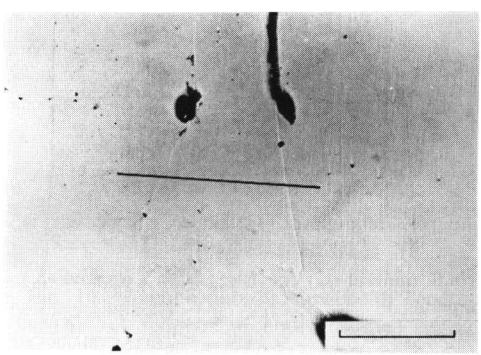

Fig. 12. Photomicrograph of a polished section of Tanakami. Kamacite plates on both sides of plessite area are swollen in shape. The line shows a electron microprobe track (See: Fig. 15). Scale bar is 0.2 mm long.

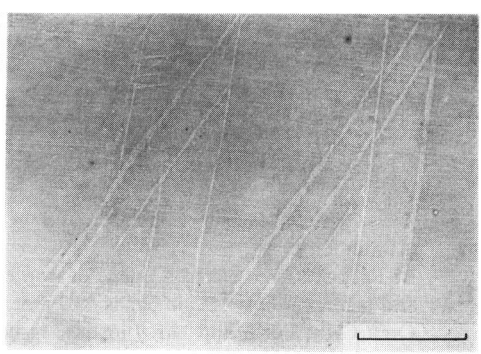

Fig. 13. Neumann bands observed in kamacite of Tanakami. Scale bar is 0.2 mm long.

Electron probe microanalysis traversing the Widmanstätten structure shows similar Fe, Ni and Co profiles to those of Kuga (Fig. 15).

Description of Tendo; In Tendo, Widmanstätten structure, being destroyed, suvives as a relic which is observed in the form of parallel or comb-shaped taenite

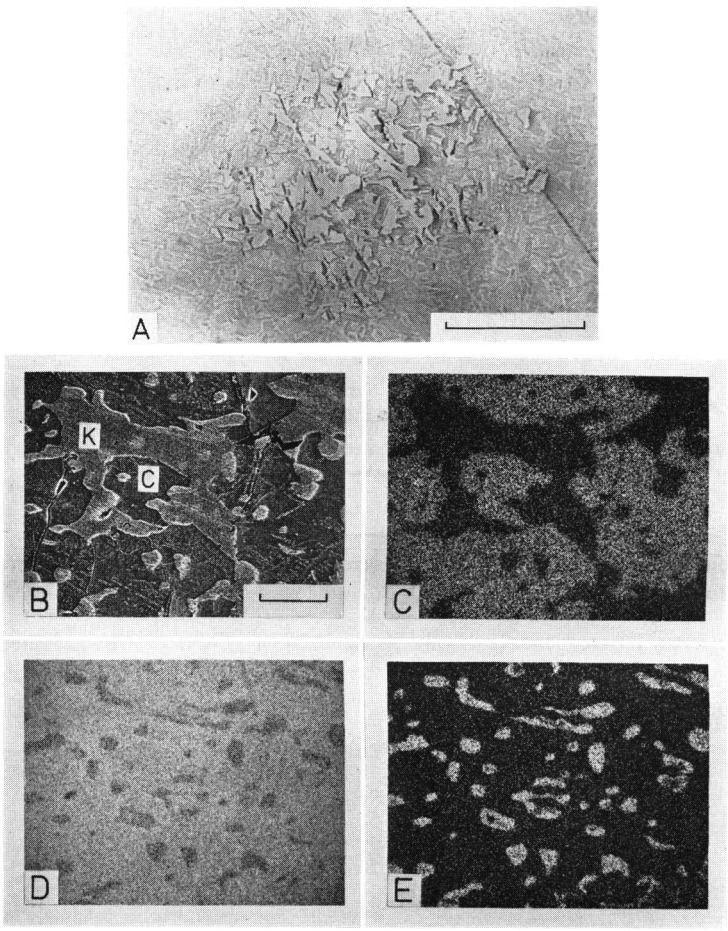

Fig. 14. A: Iron carbide mineral found in the plessite area of Tanakami. Scale bar is 0.1 mm long.
B: Back-scattered electron image of iron carbide mineral (C) coexisting with kamacite (K) and taenite grains. Scale bar is 0.02 mm long.
C–E: CKα, FeKα and NiKα images, respectively.

veins traversing the kamacite phase (Fig. 16). Magnifying a part of the taenite vein, it is observed that plessite structure has disappeared thoroughly, changing into two separated phases, kamacite and taenite, amoeboidal and spheroidal in shape (Fig. 17). The kamacite area constituting the majority of the metal phase of Tendo is made up of granular aggregates of kamacite grains, and the granulated structure is visible in the slightly weathered part, where erosion progressed along the grain sub-boundary (Fig. 18). In the kamacite phase, small rounded grains and specks of taenite are scattered. Schreibersite, 0.1 to 0.5 mm in size, is usually fractured, and a taenite halo is observed in every grain of schreibersite (Fig. 19).

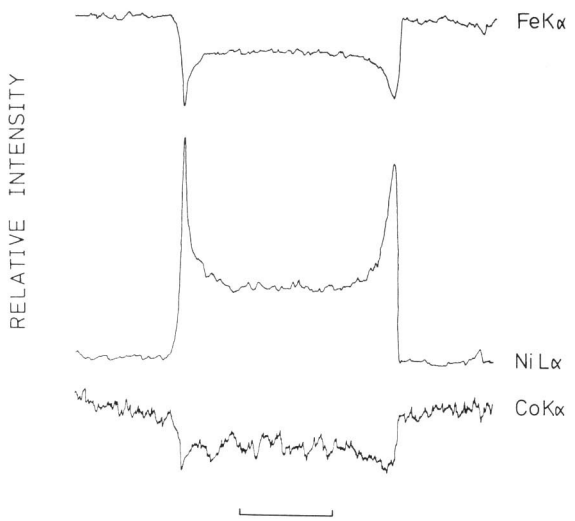

Fig. 15. FeKα, NiLα and CoKα profiles across plessite area of Tanakami in Fig. 12. Scale bar is 0.1 mm long.

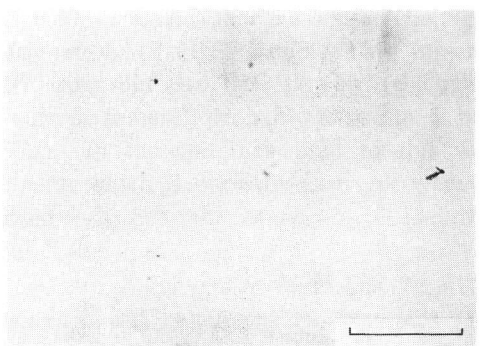

Fig. 16. Taenite veins in kamacite of Tendo. This is a remnant of Widmanstätten structure decomposed by thermal effect. Scale bar is 0.5 mm long.

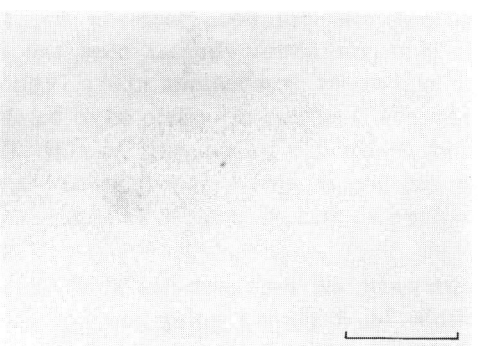

Fig. 17. A magnified view of taenite vein of Tendo. Scale bar is 0.05 mm long.

Electron microprobe profiles of Fe, Ni and Co distribution across the taenite grain in Tendo are quite different from those in the Widmanstätten structure of usual iron meteorites, and Fe, Ni and Co contents are inhomogeneous inside the grain (Fig. 20).

The structural appearance shows that the specimen of Tendo used in this examination has secondarily experienced thermal process after Widmanstätten structure was formed.

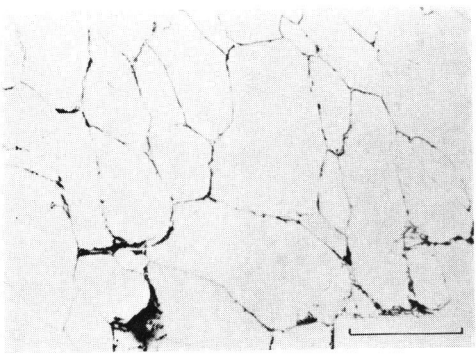

Fig. 18. Granulated structure of kamacite phase observed in the slightly weathered part of Tendo. Scale bar is 0.1 mm long.

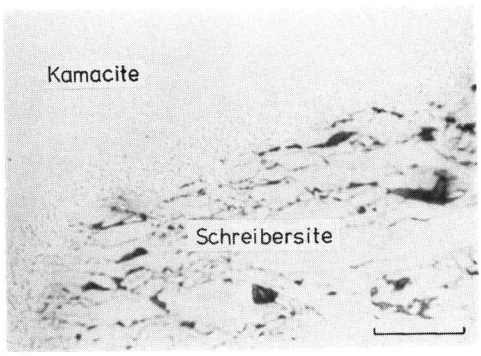

Fig. 19. Taenite rim around schreibersite grain in kamacite phase of Tendo. Scale bar is 0.02 mm long.

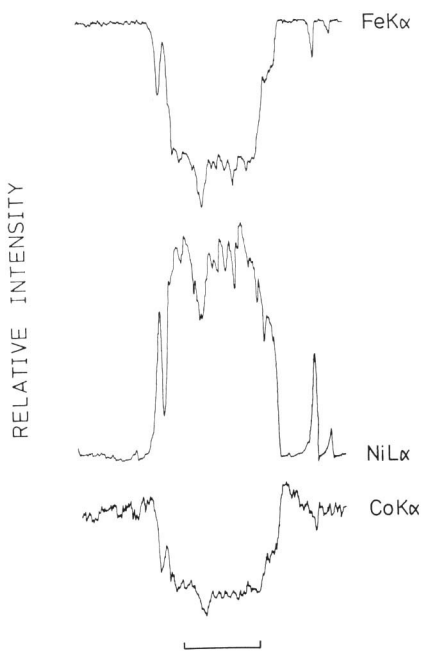

Fig. 20. FeKα, NiLα and CoKα profiles across taenite grain in Tendo. Scale bar is 0.1 mm long.

V. Discussion

From the chemical composition of Ni and P, Kuga, Shirahagi, Tanakami and Tendo were assigned to the chemical groups IIIB, IVA, IIIE and IIIA or B, respectively.

In the cases of Shirahagi and Tendo, it is difficult to discuss the correlation between the chemical classification and the structural property, because the original Widmanstätten structure is distorted or decomposed by the secondary shock or thermal effect.

In Kuga, the kamacite plate is separated from the taenite rim of plessite by the straight-lined interface, and the structural property is assigned to be Om, medium octahedrite, from the thickness of the kamacite plate. According to Wasson and Kimberlin (1967), the structural difference between IIIB iron and IIIA iron is that the kamacite plate is frequently swollen in the former and is regular in the latter. In this respect, Kuga appears different from IIIB iron. However, the Ni content of Kuga of approximately 10% is large compared with that of IIIA irons of 7.1–9.3%. The Ir content could give another judgment, that is, IIIA irons have normally much higher Ir content of 1.5–19 ppm than IIIB irons have that of 0.014–1.6 ppm. Unfortunately, however, we have not measured Ir yet. The other evidence is that lath-shaped schreibersite inclusions are frequently found in the metal phase. This is in good agreement with the properties of IIIB irons (Scott *et al.*, 1973).

Tanakami has swollen and thick kamacite plates, 1.4 ± 0.3 mm wide on average in the present specimen, and should probably be assigned to Og or Om-Og. P-Ni plots of Tanakami in this work are in favor of IIIE group rather than IIIA–B group. Because of chemical similarity between IIIE and IIIA–B irons, Scott *et al.* (1973),, stated that haxonite, $(Fe,Ni)_{23}C_6$, is a rather good indicator for the designation of IIIE group. This mineral has been recently found not only in IIIE irons but also IIIC–D irons (Buchwald, 1977). In another note on Tanakami, a carbide mineral, probably haxonite, is reported to be present in plessite (Buchwald, 1975). In the specimen used in this work, minute amounts of an iron carbide mineral which is optically isotropic were observed in plessite. This mineral is supposed to be haxonite, but is not yet identified because of the lack of chemical analysis and X-ray data.

The cooling rate of Kuga and Tanakami showing well-developed Widmanstätten structure was calculated by Wasson's (1971) equation using average band width, 0.6 mm, of kamacite and bulk Ni content 9.68% for Kuga, and 1.4 mm and 8.52% for Tanakami. The cooling rate obtained for Kuga is 1.7°C/Myr, and that for Tanakami is 1.2°C/Myr. The cooling rate of Kuga is in good agreement with that of IIIB irons of 1–2 K per million years, estimated by Goldstein and Short (1967) and Goldstein (1969). As for IIIE irons, available data to be compared with Tanakami are not found. In the case of Shirahagi exhibiting severely deformed Widmanstätten structure, the kamacite plate is described to be 0.3 mm thick on average (Buchwald, 1975). Using the Ni content of 7.68% obtained in this work, the cooling rate is calculated to be 65°C/Myr. The cooling rate of IVA irons is now in dispute, because two different data have been presented. Moren and Goldstein (1978) proposed widely different cooling rates, 3–65°C/Myr and 6–70°C/Myr, obtained by two independent methods. On the other hand, Willis and Wasson (1978) reported

cooling rates distributed in a rather narrow range of 13 to 25°C/Myr, with an average of 20°C/Myr.

Metallographic studies of iron meteorites now indicate that most of irons in chemical group III and more than half of irons in IVA are subjected to shock effect in various degrees, resulting from preterrestrial collision and break-up of the meteorite parent body or from the impact with the earth (Jaeger and Lipscutz, 1967a and b; Jain and Lipschutz, 1968 and 1970). In the present work, two meteorites, Kuga and Tanakami, exhibit the presence of Neumann bands. In Tanakami, Neumann bands are rare, while they are prevalently observed in kamacite in Kuga. According to an artificial shock-loading experiment carried on Canyon Diablo meteorite, Neumann bands are produced in the wide range of pressure of from less than 80 kb to 750 kb, and feathering of Neumann bands is observed by shocks of up to 190 kb pressure (Heymann *et al.*, 1966). As seen in Fig. 4, the feathering is noticed in the well-polished surface of kamacite in Kuga, but the features which are produced by higher shocks, *i.e.*, well-developed hatching of Neumann bands, ε-iron formation and shock-induced recrystallization, are not observed in the present specimen. Applying the classification of shock intensity proposed by Heymann *et al.* (1966), Kuga is considered to be a moderately shocked meteorite and Tanakami is probably a lightly shocked one. Although Tendo belongs to III group iron, it is structurally different from Kuga and Tanakami. The structural appearance of this meteorite showing a remnant of Widmanstätten structure and no Neumann bands cannot be accounted for by a shock-induced effect. It is rather believed that the present specimen of Tendo has been influenced by a postformational thermal process. The microscopic features showing decomposed taenite bands and spheroidic taenite grains dispersed in kamacite are very similar to the structure of Maria Elena and Seneca Falls which are assumed to have undergone an extraterrestrial annealing (Buchwald, 1975).

The occurence of taenite-rimmed schreibersite grains in kamacite is interesting in estimating the heating temperature. Heat treatment of the Canyon Diablo meteorite carried out by Brentnall and Axon (1962), has ascertained that taenite halos are formed around schreibersite grains by migration of nickel into kamacite at a temperature ranging up to 900°C. This feature agrees well with the microscopic feature seen in the present sample of Tendo, and suggests that Tendo has been secondarily heated up to 900°C at most after the formation of Widmanstätten structure. If cohenite could be found in Tendo, the secondary heating effect could be more definitely confirmed by the presence of the reaction at the interface between cohenite and kamacite. However, it is not conclusive whether Tendo has been affected by a thermal process in the extraterrestrial environment. It is also probable that the thermal effect observed in the present study was caused by heating during the descent in the atmosphere of the earth, because our Tendo specimen was cut from the part near the surface of the main mass.

The peculiar feature of Shirahagi showing a distorted internal structure and a

curved external appearance seems to be due to very extensive deformation which it suffered from either a preterrestrial shock event or impact with the ground on the earth. The microscopically observed structure is quite similar to that of cold-worked, hammered iron alloys. A note on Shirahagi by Buchwald (1975) favors a cosmic shock event. However, considering the geographical location where Shirahagi fell, another interpretation is possible that the meteorite was greatly deformed into a Japanese-helmet-like shape while rolling down and crushing bumping and striking against terrestrial huge stones in the mountainous river, just like a big and violent water fall, after falling on the earth.

VI. Conclusion

The chemical composition of Fe, Ni, Co, P, Cu and Cr of four Japanese iron meteorites, Kuga, Shirahagi, Tanakami and Tendo has been determined. From correlation between P and Ni, Kuga, Shirahagi, Tanakami and Tendo are considered to belong, respectively, to chemical groups IIIB, IVA, IIIE and IIIA or B. The cooling rates of Kuga and Tanakami are estimated to be 1.7°C/Myr and 1.2°C/Myr, respectively, differing by bulk Ni content and kamacite band width. Microscopic examination of structure and minerals shows that Kuga and Tanakami have gone through a post-formational thermal process.

References

Brentnall, W. D. and H. J. Axon, 1962. The response of Canyon Diablo meteorite to heat treatment. *J. Iron Steel Inst.* **200**: 947–955.

Buchwald, V. F., 1975. Handbook of Iron Meteorites. University of California Press. Berkley, Los Angeles, London.

———, 1977. The mineralogy of iron metorites. *Phil. Trans. Roy. Soc. London* **A286**: 453–491.

Enomoto, T., 1902. Note on the swords made of meteoritic iron. *J. Geography (Japan)* **14**: 33–39. (in Japanese)

Goldstein, J. I., 1969. The classification of iron meteorites. *In* Meteorite Research, (editor P. M. Millman) pp. 721–737. Reidel.

———, and J. M. Short, 1967. Cooling rates of 27 iron and stony-iron meteorites. *Geochim. Cosmochim. Acta* **31**: 1001–1023.

Heymann, D., M. E. Lipschutz, B. Nielsen and E. Anders, 1966. Canyon Diablo meteorite: Metallographic and mass spectrometric study of 56 fragments. *J. Geophys. Res.* **71**: 619–641.

Imai, S., W. Aihara, H. Mizukami, Y. Omori and T. Masuda, 1978. Shimadzu inductively coupled plasma quantometer model ICPQ-100. *Shimadzu Review* **35**: 59–63. (in Japanese with English summary)

Jaeger, R. H. and M. E. Lipschutz, 1967a. Pressure history of some iron meteorites. *Nature* **213**: 975–977.

——— and ———, 1967b. Implications of shock effects in iron meteorites. *Geochim. Cosmochim. Acta* **31**: 1811–1832.

Jain, A. V. and M. E. Lipschutz, 1968. Implications of shock effects in iron meteorites. *Nature* **220**: 139–143.

——— and ———, 1970. On preferred disorder and the shock history of chemical group IVA meteorites. *Geochim. Cosmochim. Acta* **34**: 883–892.

KŌ, S., 1899. Iron meteorite, rare in this world. *J. Geol. Soc. Japan* **6**: 446–448. (in Japanese)

KONDO, K., 1895. Iron meteorite found in Toyama Prefecture. *J. Geography (Japan)* **7**; 274–276. (in Japanese)

MOREN, A. E. and J. I. GOLDSTEIN, 1978. Cooling rate variations of group IVA iron meteorites. *Earth Planet. Sci. Letts.* **40**: 151–161.

MURAYAMA, S., 1953. The peculiar structure of the Shirahagi, Japan, Siderite (CN=±1375.367). *Meteoritics* **1**: 99–102.

———, 1959. The Kuga, Japan, Siderite. *Bull. Nat. Sci. Mus.* **4**: 359–366.

———, 1965. The main mass of "Kuga" iron meteorite. *Natural Science and Museums* **32**: Nos. 3–4, 46–49. (in Japanese)

———, 1977. Two new meteorites from Yamagata-ken. National Science Museum News Sept. p. 6. (in Japanese)

OTSUKI, Y., 1900. Iron meteorite in Tanakami Mountain, Ohmi Province. *J. Geol. Soc. Japan* **7**: 85–93. (in Japanese)

SCOTT, S. R. D., J. T. WASSON and V. F. BUCHWALD, 1973. The chemical classification of iron meteorites-VII. A reinvestigation of irons with Ge concentrations between 25 and 80 ppm. *Geochim. Cosmochim. Acta* **37**: 1957–1983.

SHIMA, Masako, 1964. The distribution of germanium and tin in meteorites. *Geochim. Cosmochim. Acta* **28**: 517–532.

———, and M. HONDA, 1966a. Distribution of spallation produced chromium between alloys in iron meteorites. *Earth Planet. Sci. Letts.* **1**: 65–74.

———, and ———, 1966b. Isotopic measurements of chromium induced by cosmic-rays in iron meteorites. *Shitsuryo Bunseki (Mass Spectroscopy)* **14**: 23–34. (in Japanese with English summary and table and figure captions)

WASSON, J. T., 1971. An equation for the determination of iron meteorite cooling rates. *Meteoritics* **6**: 139–148.

———, 1974. Meteorites, classification and properties. Springer-Verlag, Berlin, Heidelberg, New York.

———, and J. KIMBERLIN, 1967. The chemical classification of iron meteorites-II. Irons and pallasites with germanium concentrations between 8 and 100 ppm. *Geochim. Cosmochim. Acta* **31**: 2065–2093.

WILLIS, J. and J. T. WASSON, 1978. Cooling rates of group IVA iron meteorites. *Earth Planet. Sci. Letts.* **40**: 141–150.